



Implementation of Synthetic Aperture Radar Active Decoy Hardware

S. A. Elgamel^{1*}, M. Hanafi² and M. S. Abdel-Latif¹

¹ Military Technical College, Cairo, Egypt

² Egyptian Armed Forces, Cairo, Egypt

The manuscript was received on 6 June 2022 and was accepted after revision for publication as research paper on 23 November 2022.

Abstract:

As a result of the military's use of synthetic aperture radar (SAR), it has become necessary to use jamming techniques to protect sensitive sites of friendly forces from being intercepted by SAR. To combat SAR sensors, two jamming techniques are typically available: noise jamming and deceptive jamming. In this paper the design and hardware implementation of a proposed active decoy which works as deceptive jamming system, is achieved using field programmable gate array (FPGA). The performance of the developed system is evaluated by SystemVue. 2015.01, using "hardware in the loop" methodology.

Keywords:

active decoy, FPGA, SAR

1 Introduction

The amazing technological development in radar and electronic warfare systems has led to complexities in the simulation of these fields [1]. Searching for a new test platform methodology for designing and verifying SAR model, a system level design tool, called SystemVue has proposed the solution [2]. SystemVue can achieve multiple scenarios for a complex radar, electronic warfare systems simulation environment to generate complex waveforms for the transmitters and receivers of radar. Moreover, it can be used to generate electronic warfare waveforms with clutter, interference, and jamming to provide advanced measurements for system performance evaluation. SystemVue acts as an intermediate stage between simulation world, as in Matlab; and the real implementation world, as in field programmable gate array (FPGA). It can handle

* Corresponding author: Electronic Warfare Department, Military Technical College, Kobri Elkobba, Cairo, Egypt. Phone: +202-22 62 19 08, E-mail: elgamel@mtc.edu.eg. ORCID 0000-0003-0627-5729.

a hardware in the loop (HIL), to get the simulation out into the manufacturing world [3].

SHU et al. present a novel implementation of real-time radar environment simulator with four channels for missile-borne SAR using wideband DRFM technique and parallel computing technique based on FPGA is presented. This simulator provides real-time computation capability for raw SAR echo signal generation of extended scenes with a very small computational delay [4]. In [5], based on digital radio frequency memory (DRFM) technology, radar jammer can copy the radar signal multiple times with different time delay and frequency shift to form dense false targets jamming in the time domain. For non-self-protection type jamming, a two dimensional dense false targets can be formed by multiple jammers which has a great influence on radar angle and range measurement. The analyses of the formation mechanism of dense false target jamming in the time and spatial domain are presented. The effectiveness of the method is verified by Matlab simulation. In [6], the inverse RDA (IRDA) deception jamming technique and its evaluation criteria on SAR are demonstrated. Mathematical formulations for SAR RDA with and without deception jamming are presented. In addition, Matlab simulation and results of SAR RDA under the proposed deception scenario are discussed. SAR point target simulation of the proposed deceptive jamming and false target insertion into real large scene are also introduced. Comparison of the proposed deceptive jamming to signal power ratio (JSR) required to counter SAR with other SAR jamming techniques is analyzed.

In this paper, three main objectives are achieved. The first objective was to confirm that the same SAR output results are achieved if the predesigned Matlab SAR model in [6] replaces the built-in SystemVue SAR model. These modifications are performed due to the limitations in the built in block diagram of SAR in SystemVue. These modifications enable more control capabilities to the available built in SAR model in SystemVue ver. 2015.01. The second objective, the deceptive jamming against modified SystemVue SAR model with Matlab based approach is also presented to ensure that the same SAR output results, under deception jamming signal, are achieved if the predesigned Matlab SAR model replaces the built-in SystemVue SAR transmitter model. The third objective was the hardware implementation of the proposed active decoy against SAR using Xilinx AKC705 Kintex-7 FPGA board. The different modules of the implementation of the proposed active decoy are explained. The performance of proposed jammer against SAR model is displayed using HIL methodology.

The paper is organized as follows: the SAR model in SystemVue, in addition to the deceptive jamming against SystemVue SAR model, are demonstrated in section 2. Section 3 demonstrates the implementation of the active decoy against SAR using Xilinx Kintex-7 FPGA board. In section 4, the performance evaluation of the proposed active decoy against SAR model using HIL methodology is performed. Section 5 demonstrates the simulation and results of this paper. The conclusion of this paper is shown in section 6.

2 SAR Models and the Deceptive Jamming Signal

The range Doppler algorithm (RDA) [7] is one of the most commonly utilized algorithms in the image formation processor (IFP) for processing continuously collected data into an image [8]. It compresses the raw data using the matched filter in the fast and slow time dimensions. RDA corrects for the range cell migration (RCMC) in the

range Doppler domain [9]. SystemVue platform simplifies the design and test of Radar/EW systems, while offering a number of key benefits, including the ability to generate complex waveforms for transmitters, receivers and EW system test. SystemVue platform can also introduce radar/EW environments including clutter, interference, and jamming/deception with advanced measurements for system performance evaluation.

2.1 SAR model in SystemVue Ver. 2015.01

The adopted SAR model, in SystemVue uses the RDA. The block diagram of the SAR model is built on SystemVue Ver. 2015.01, as shown in Fig. 1.

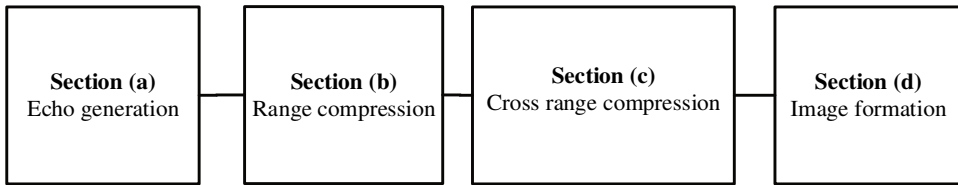


Fig. 1 Simulation block diagram of SAR using SystemVue

This model can handle single or multiple point targets, however, it is limited in handling image targets (the proposed solution to deal with image targets will be discussed in section 2.2). In Fig. 2 the block diagram of the SAR model, in SystemVue, consists of four main sections a, b, c, and d. In section (a), the raw data generation part is simulated. In section (b), range compression process is carried out on the SAR echo signal, by the range compression filter. In section (c), cross range (azimuth) compression is performed similar to range compression, using cross range compression filter. The formation of the image is performed in section (d). The SAR model in SystemVue ver. 2015.01 is shown in Fig. 2.

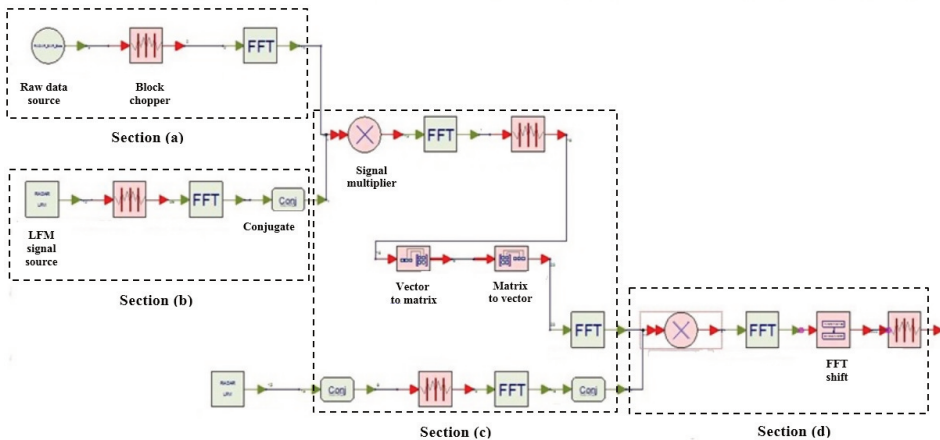


Fig. 2 The SAR model in SystemVue ver. 2015.01

2.2 Modified SAR model in SystemVue Ver. 2015.01

Several modifications are done to SAR model in SystemVue ver. 2015.01 to handle image targets. The modified SystemVue ver. 2015.01 block diagram main components

will be discussed in details as following. The transmitter raw data is replaced with a Matlab script block, thus it allows controlling different SAR parameters. These parameters can be controlled using the interface windows of SystemVue. Some other parameters related to the generated echo signal are controlled in the Matlab code, such as SAR matrix size, and the location of the target inside the image. Thus, the modified SystemVue SAR model generate the SAR raw data with more powerful controlling tools.

Raw data signal based Matlab approach: Fig. 3 shows raw data generation. In Fig. 3a, the raw data generation based SystemVue ver. 2015.01 is presented and the modified raw data generation based Matlab approach is seen in Fig. 3b. The typical SAR parameters of the generated raw data signal will be shown later in the results and simulations section.

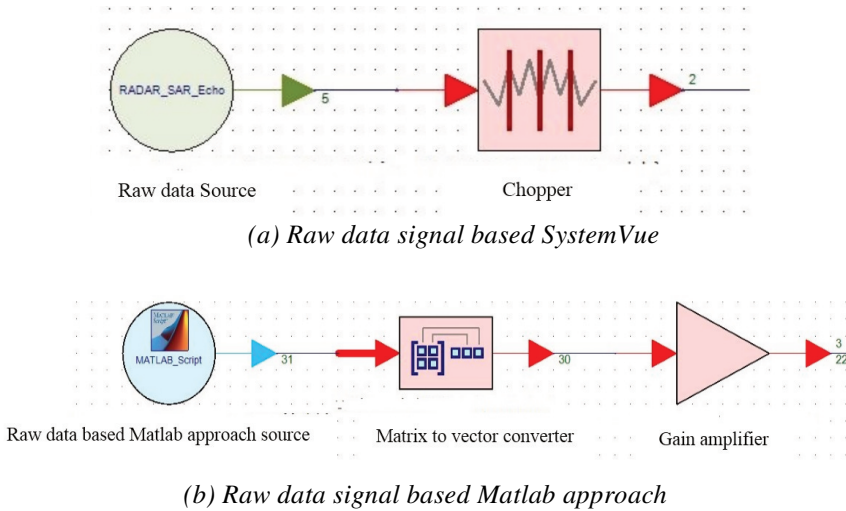


Fig. 3 Raw data generation

The generated signal, the SAR received signal $S_r(\tau, \eta)$ from a point target, is expressed as [10]:

$$S_r(\tau, \eta) = A_o w_r \left[\tau - 2R(\eta) \right] w_a(\eta - \eta_c) \exp \left\{ -\frac{j4\pi f_o R(\eta)}{c} + j\pi K_r \left[\tau - \frac{2R(\eta)}{c} \right]^2 \right\} \quad (1)$$

where A_o is an arbitrary complex constant, τ is the time delay related to range dimension, η is the azimuth time referenced to closest approach, η_c is the beam center offset time, $w_r(\tau)$ is the range envelope (rectangular function), $w_a(\eta)$ is the azimuth envelope (Sinc squared function), f_o is the SAR center frequency, K_r is the range chirp FM rate, $R(\eta)$ is the instantaneous slant range, j is the imaginary number, and c is the microwave propagation speed.

Reference signal in range and cross range (Azimuth) dimensions based Matlab: Fig. 3b shows the block diagram of generation of reference signal in range dimension using Matlab script. It replaces the reference signal generation in SystemVue SAR model, shown in Fig. 3a. Using Matlab script, range Doppler algorithm firstly compresses the data in the range dimension via matched filter implemented in frequency domain by multiplying the one dimensional range Fourier transform of the

input raw data with the Fourier transform of the generated reference signal which represents the matched filter frequency response. The frequency domain range compression matched filter $G(f_r)$, is expressed as [11]:

$$G(f_r) = \text{rect}\left(\frac{f_r}{K_r T}\right) \exp\left(-j\pi \frac{f_r^2}{K_r}\right) \quad (2)$$

where $\text{rect}()$ is a rectangular function, f_r is the signal frequency in the range dimension, and $K_r T$ is the time bandwidth product, K_r is the FM rate in the range dimension, and T is the chirp duration.

After range compression, the range compressed signal will get compressed also in the azimuth (cross range) dimension via another frequency domain matched filter process. It is obtained by multiplication of one dimensional range azimuth Fourier transform of the range compressed signal with the Fourier transform of the azimuth reference function which represents the matched filter frequency response. The azimuth matched filter in frequency domain, $H_{az}(f_\eta)$, can be expressed according to [11]:

$$H_{az}(f_\eta) = \exp\left(-j\pi \frac{f_\eta^2}{K_a}\right) \quad (3)$$

where K_a is the FM rate in the azimuth direction, and f_η is the signal frequency in the azimuth dimension.

2.3 Deceptive Jamming against SystemVue SAR model

To deceive SAR, a spurious scene or target is introduced to its focused image. SAR active decoy receives the return SAR echo from the protected area, and measures its (kinematic, antenna, and signal) parameters, and transmits that signal back to SAR, after making the deception process on it. The spurious scene or target is converted into deceptive jamming signal [12]. The generation steps of the deceptive jamming signal based on the inverse range Doppler algorithm is presented in [13].

The deceptive jamming signal (generated using code in a Matlab script) is added to the modified SAR model based Matlab approach (described in the previous section). The deceptive jamming signal $s_{\text{rec}}(\tau, \eta)$ is expressed as [6]:

$$s_{\text{rec}}(\tau, \eta) = (A_j + A_r) \left[\begin{array}{c} w_r \left[\tau - \frac{2R_j(\eta)}{C} \right] w_a (\eta - \eta_c) \cdot \\ \exp \left\{ -j4\pi f_o \frac{R_j(\eta)}{c} + j\pi K_r \left[\tau - \frac{2R_j(\eta)}{C} \right]^2 \right\} \end{array} \right] + n(\tau, \eta) \quad (4)$$

where A_j and A_r are the arbitrary complex constant related to the jamming signal amplitude, $n(\tau, \eta)$ is the SAR internal noise, and $R_j(\eta)$ the jammer instantaneous slant range.

The idea of introducing the deceptive jamming into SAR scene using SystemVue models is presented in Fig. 4. There are two main dashed blocks from which the upper dashed block is responsible for generating the target echo and the lower is responsible for generating the deceptive jamming signal using the modified SAR model in SystemVue. Thus, the deceptive jamming signal is added to the target echo in this model.

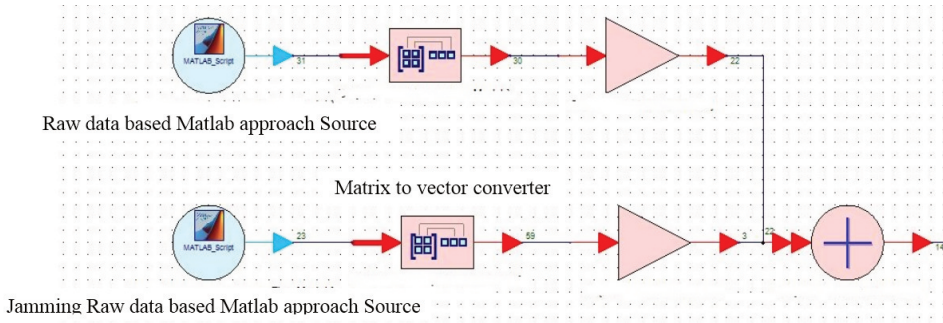


Fig. 4 Block diagram of deceptive jamming against SAR in SystemVue

3 Jammer Implementation Using Xilinx Kintex-7 FPGA Board

The block diagram of the hardware implementation of the proposed active decoy is shown in Fig. 5. The SAR reference signal matrix is correlated with the generated deceptive image data matrix to produce the SAR jamming signal. The correlation process is performed in frequency domain.

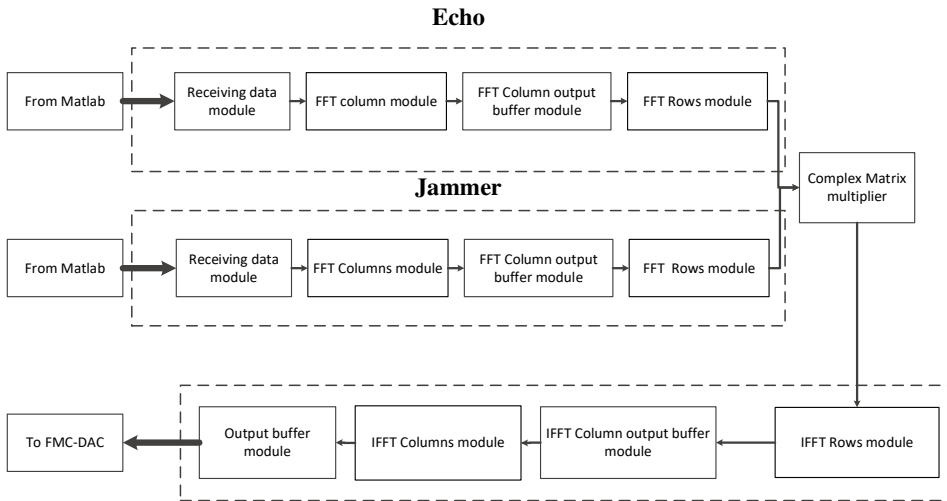


Fig. 5 Block diagram of hardware implementation of active decoy

This figure contains three main dashed blocks. The upper dashed block is responsible for converting the received SAR signal, which has been generated previously based on a software Matlab program, from time domain into frequency domain. In the same way, the middle dashed block is responsible for generating the frequency domain deceptive image data. The outputs of the upper and middle dashed blocks are multiplied and then fed to the lower dashed block. This block is responsible for producing the time domain SAR digital jammed signal. This signal is then fed to the data acquisition board (FMC 150-DAC) to form the SAR analogue jammed signal. The functionality of each block of this figure is explained as follows.

Receiving data module: It is a block memory written in VHDL code and it is used to store the complex data of the reference signal or the deceptive image. These

data are generated by Matlab programs and stored in two read only memories (ROMs). The dimension of each data matrix is $N_a \times N_r$, where N_a is the number of samples in the azimuth dimension and N_r is the number of samples in the range dimension. The width of each sample is 10 bits.

Fast Fourier transformation and inverse fast Fourier transformation modules: These modules are built based on FFT Xilinx intellectual property core V7.1. This core computes an N -point forward FFT or inverse FFT (IFFT). The parameters of FFT or IFFT cores for column or raw process are shown in Tab. 1.

Tab. 1 FFT/IFFT column and raw modules' parameters

Parameter	FFT column	FFT raw	IFFT raw	IFFT column
Clock frequency [MHz]	200	200	200	200
Input data width [bits]	10	15	34	39
Output data width [bits]	15	15	39	39
Phase factor width [bits]	8	8	8	8

FFT column output buffer module: This module is written in VHDL code. It takes the values of the data from the FFT column module and stores them in a temporary buffer. The data is then rearranged in the form of rows to be ready for performing the raw FFT. The width of the input or output data samples is 15 bits.

Complex matrix multiplier module: This module is written in VHDL code and it performs the multiplication process of two complex matrices. The first matrix is the data of the reference signal, after performing the 2-D FFT. The second matrix is the deceptive image data, after performing the 2-D FFT. The output data width of this module is 34 bits.

IFFT column output buffer module: This module is written in VHDL code. It receives the values of the data from the IFFT raw module and stores them in a temporary buffer. The data is then rearranged in the form of columns to be ready for performing the second dimension IFFT. The size of the input or output data is 39 bits.

Output buffer module: This module is written in VHDL code. It receives the data from the IFFT column module, stores it in a ROM, and rearranges it in a form of a matrix to be acquired by the data acquisition board (FMC150). The input data width of this module is 39 bits. The output data width from this module is taken to be 16 bits to be suitable to the used data acquisition board.

4 Jammer Performance Using “HIL” Methodology

SystemVue has an advantage of integration into hardware design, and verification flows. The SystemVue HIL co-simulation engine allows the dynamic use of FPGA hardware. HIL methodology allows to accelerate computational tasks in a multi-threaded software environment. SystemVue HDL co-simulation simulates components represented in a HDL, VHDL and Verilog, in the same schematic with other SystemVue components [14]. This integrated capability provides complete design flexibility and complements other SystemVue features, including HDL generation.

4.1 Extra Modified SAR Model in SystemVue Ver. 2015.01 due to HIL

The SAR model in SystemVue is extra modified to be able to work with acquired analog signal from FMC card that concocted to AKC705 Kintex-7 FPGA board. It is required to replace the simulated active decoy by Matlab based approach with victor signal analyzer VSA 89600 to be able to acquire the deceptive raw data generated from the AKC705 Kintex-7 board, and acquired by DSO9104A wide band oscilloscope, as shown in Fig. 6.

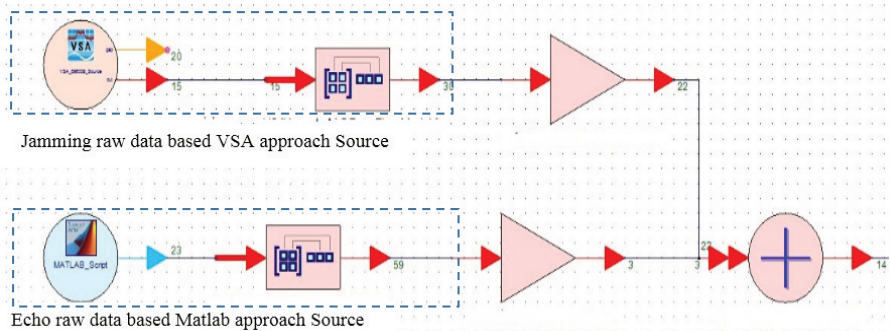


Fig. 6 SAR model modified to HIL

4.2 Implementation of HIL Methodology

Fig. 7a shows the configuration of the HIL consisting of A KC705 Kintex-7 board (it is used to emulate the jammer) in which the VHDL code is downloaded. The output of the kit is acquired to the DSO9104A wideband oscilloscope (it is used to emulate the SAR RF front end) through FMC 150 4 DSP DAC data acquisition card. The Implemented SAR active decoy on A KC705 Kintex-7 board should be connected to the SAR model on SystemVue through VSA_89600. A real picture of this setup HIL in shown in Fig. 7b.

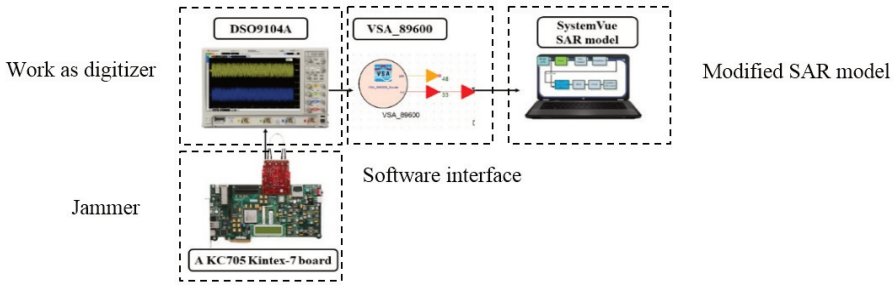
5 Simulations and Results

In order to implement the active decoy on Xilinx AKC705 Kintex-7 FPGA board, it is required to use SystemVue as a test platform. Thus, a group of simulation and emulation tests are done as follows: firstly, a simulation to confirm that the same SAR output results are achieved if the predesigned Matlab SAR model in [6] replaces the built-in SystemVue SAR model; secondly, a simulation of the deceptive jamming against modified SystemVue SAR model (with Matlab based approach) to ensure that the same SAR output results, under deception jamming signal, are achieved; finally, an emulation of the proposed active decoy against SAR using Xilinx AKC705 Kintex-7 FPGA board. The results are demonstrated in different types of Matlab figures and graphs.

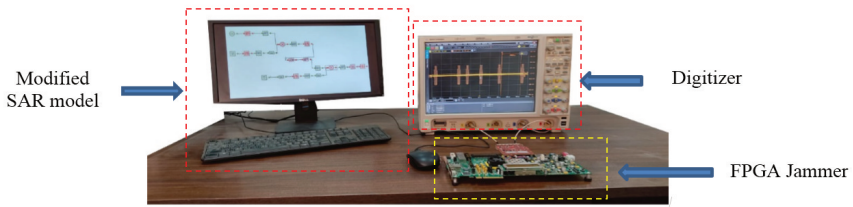
5.1 Simulation of Modified SystemVue SAR Model

In this section, the simulation is described which has been done to ensure that the same SAR output results are achieved if the predesigned Matlab SAR model replaces the built-in SystemVue SAR model transmitter. Modifications to SystemVue SAR model with Matlab based approach has been performed (SAR is considered to capture an

image target). The SAR processed image is of Giza pyramids area, it is a SAR focused image by courtesy of ASI, and E-Geos [15]. The generated raw data of the image target is shown in Fig. 8a. The considered simulation parameters are shown in Tab. 2. Fig. 8b shows the SAR image plot of Giza pyramids area by the modified block diagram of SAR model and it is the same result as the one archived previously in [6].

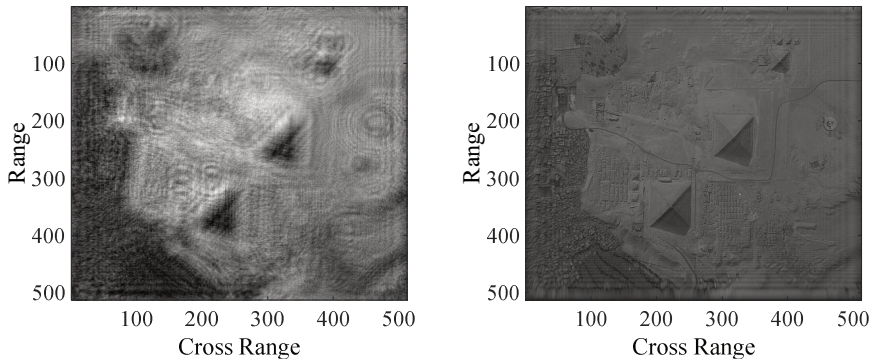


a) Schematic diagram of HIL configuration



b) Real picture of HIL configuration

Fig. 7 HIL Configuration



a) SAR raw data for image target

b) Image plot of Giza pyramids

Fig. 8 SAR Image Plot of Giza pyramids [15] (1 m/pixel spatial resolution)

5.2 Simulation of Deceptive Jamming against SystemVue SAR Model

This section presents the simulation which was done to ensure that the same SAR output results, under deception jamming signal, are achieved if the predesigned Matlab SAR model replaces the built-in SystemVue SAR model transmitter. The point target

simulation has been used to proof the deception concept using the modified SystemVue SAR model. In this simulation, the SAR target is considered as multiple points located in certain locations (three targets No. 1, 2, and 3) and another deceptive point is inserted into the image as a spurious target (one targets No. 4); these points are listed in Tab. 3. Thus, the total received raw data at the SAR receiver front end consists of a mix of two types of raw data. It contains the original targets raw data, in addition to the raw data of the inserted spurious target image.

Tab. 2 SAR parameters in modified SystemVue SAR model

Parameter	Value
Carrier frequency	10 GHz
Chirp pulse duration	3 μ s
Transmitted bandwidth	200 MHz
Pulse repetition frequency (PRF)	1.5 kHz
Effective antenna dimension along azimuth direction (L_a)	0.5 m
Effective antenna dimension along range direction (L_r)	0.2 m
SAR platform moving speed	250 m/s
SAR height	1.4 km

Tab. 3 Targets Coordinates

Target No.	Coordinate	
	N_a	N_r
1	256	128
2	128	384
3	384	384
4	355	355

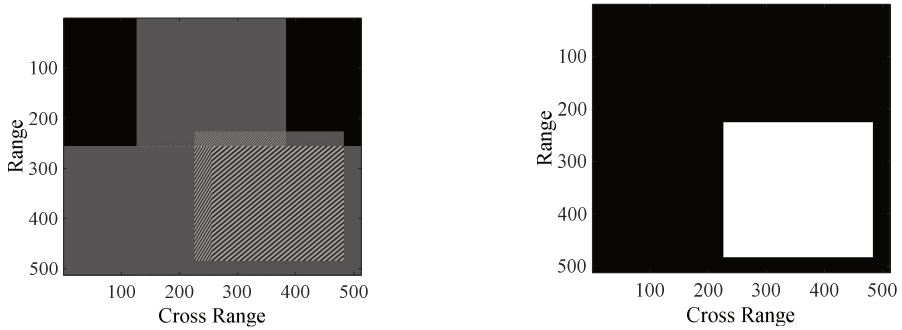
Fig. 9a shows the raw data for the three original targets and Fig. 9b shows the raw data for the deceptive added target (spurious point target). The 3D Plot of SAR image under deceptive jamming is shown in Fig. 9c and the SAR focused image of the received raw data is shown in Fig. 9d for three original points, in addition to the inserted deceptive point target.

Mean absolute difference (MAD) [16, 17] in digital image processing is a measure of the similarity between image blocks. It is used in [6] to reflect the difference of the two images with and without jamming. MAD at different values of jamming to signal ratio (JSR) is listed in Tab. 4.

5.3 Active Decoy against SAR Model Using “HIL” Methodology

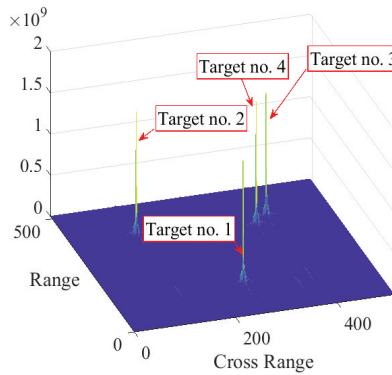
This section shows the emulation of SAR with applying deceptive jamming generated from AKC705 Kintex-7 board, which has been applied to SAR model in SystemVue using HIL. SAR is considered to be working in a strip-map mode, with no. of samples in azimuth ($N_a = 16$), and no. of samples in range ($N_r = 16$). Fig. 10 shows the generated SAR raw data for the point target which is located in SAR focused image in

($N_a = 10$), and ($N_r = 10$). The emulation parameters are listed in Tab. 5, some of them have been chosen to be as near as possible to the real SAR signal parameters values to meet the hardware limitations of Xilinx AKC705 Kintex-7 FPGA board.

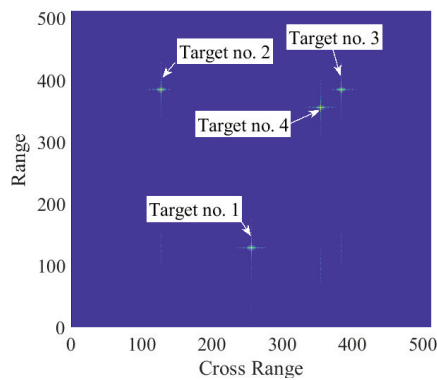


a) Three point targets raw data

b) Deceptive point target raw data



c) 3D Plot of three point targets and one deceptive point target



d) 2D Plot of three point targets and one deceptive point target

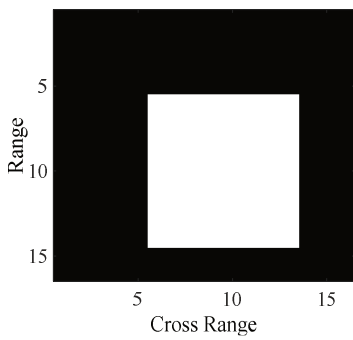
Fig. 9 SAR image plot under deceptive jamming (1 m/pixel spatial resolution)

Tab. 4 Evaluation of point insertion effect in smart deceptive jamming using MAD

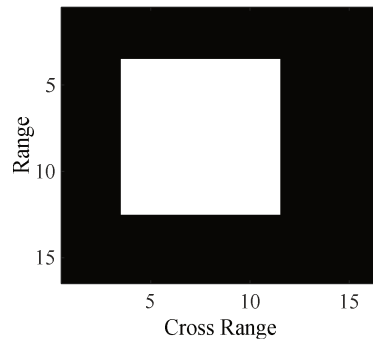
JSR [dB]	-8	-5	-3	0	3	5	8
MAD	165.5	232.4	425.5	695.5	1120.5	1398.87	1785.27

Tab. 5 The emulation parameters of SAR in SystemVue using HIL

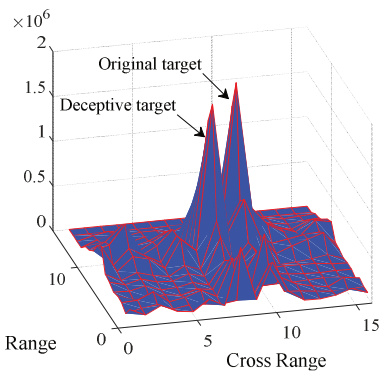
Parameter	Value
Carrier frequency	10 GHz
Chirp pulse duration	4 s
Transmitted bandwidth	1000 Hz
LFM rate	1.4 Hz/s
Effective antenna dimension along azimuth direction (L_a)	0.5 m
Effective antenna dimension along range direction (L_r)	0.2 m
SAR platform moving speed	200 m/s
SAR height	83 m



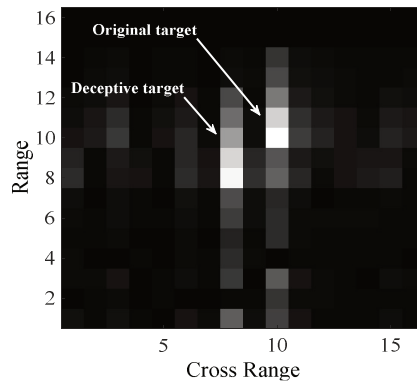
a) Raw Data for point Target



b) FPGA Raw Data point Target



c) 3D SAR image



d) SAR image (range and cross range)

Fig. 10 SAR image plot under FPGA active decoy (1 m/pixel spatial resolution)

The raw data of the appointed target of SAR is shown in Fig. 10a while Fig. 10b shows the generated raw data which was then passed to the range compression filter. This raw data is multiplied with the generated reference in range. The output of the range compression filter was then passed to the cross range (azimuth) matched filter. It was correlated with the generated reference signal. Fig. 10c shows the 3D plot of the SAR focused image for point target. Fig. 10d shows the SAR image plot for the point target, located in the coordinates ($N_a = 10$, $N_r = 10$), and the generated FPGA deceptive jamming point target located in ($N_a = 8$, $N_r = 8$).

Tab. 6 shows the values of MAD at different values of JSR to evaluate point target deceptive jamming effect using FPGA.

Tab. 6: Evaluation of point target deceptive jamming effect using FPGA

JSR [dB]	-8	-5	-3	0	3	5	8
MAD	142.9	264.5	456.9	758.8	1123.5	1425.9	1875.2

It is clear from the hardware implementation of the proposed deceptive jammer using Xilinx AKC705 Kintex-7 FPGA board (in the laboratory level) that the concept of applying the proposed method in a real SAR active decoy is applicable. It is accomplished by feeding the DRFM (active decoy core) by the victim SAR parameters (from the integrated electronic support measures systems) and the required deceptive image of the protected area. The active decoy generates a coherent deceptive raw data and transmits it to the victim SAR.

6 Conclusion

This paper has introduced SystemVue as a test platform methodology. SAR model in SystemVue ver. 2015.01 is a limited model, thus it can handle only point target or multiple point's target. Therefore, modifications to that model using Matlab based approach were performed resulting in the modified model which can handle image target as well as point target or multiple point's target. Point target simulation of the deceptive jamming against SAR focused image using SystemVue was performed. In addition, simulation of false target insertion into SAR focused image using SystemVue was performed. A hardware implementation of the proposed active decoy against SAR using Xilinx Kintex-7 FPGA board was emulated. The HIL methodology was used to evaluate the performance of the hardware implementation of the proposed active decoy.

References

- [1] SEVGI, L. Radar Simulation. In: SEVGI, L. *Complex Electromagnetic Problems and Numerical Simulation Approaches*. Wiley-IEEE Press, 2003, pp. 309-352. DOI 10.1109/9780470544280.ch6.
- [2] WANG, Z., H. HAN, M. LIU and Q. YANG. Modeling and Simulation of Pulse Doppler Radar System Based on Systemvue Code. In: *2017 International Applied Computational Electromagnetics Society Symposium (ACES)*. Suzhou: IEEE, 2017, pp. 1-2. ISBN 978-1-5090-4311-8.
- [3] VASANI, J., T. KUMAR, R. NAGPAL, M. NAIK and R. MALIK. Baseband OFDM Physical Layer Implementation on FPGA Using SystemVue. In: *2016 International Conference on Wireless Communications, Signal Processing and*

- Networking (WiSPNET)*. Chennai: IEEE, 2016, pp. 967-972. DOI 10.1109/WiSPNET.2016.7566278.
- [4] SHU, T., B. TANG, K. YIN, Q. SUN, Y. CHEN and W. YU. Development of Multichannel Real-Time Hardware-in-the-Loop Radar Environment Simulator for Missile-Borne Synthetic Aperture Radar. In: *2015 IEEE Radar Conference (RadarCon)*. Arlington: IEEE, 2015, pp. 0368-0373. DOI 10.1109/RADAR.2015.7131026.
- [5] LIU, K., X. FU, Z. GAO and D. LI. Time-Space Two-Dimensional Dense False Targets Jamming and Countermeasures. In: *2018 13th IEEE Conference on Industrial Electronics and Applications (ICIEA)*. Wuhan: IEEE, 2018, pp. 1982-1987. DOI 10.1109/ICIEA.2018.8398034.
- [6] ELGAMEL, S.A. and M.S. ABDEL-LATIF. Synthetic Aperture Radar Active Decoy. *Advances in Military Technology*, 2022, **17**(1), pp. 47-62. DOI 10.3849/aimt.01520.
- [7] WANG, Z., Y. LI, S. SHAO, S. LI, J. XIAO, J. and J. WU. Improved Range Doppler Algorithm Based on Squint FMCW-SAR. In: *12th International Conference on Signal Processing and Communication Systems (ICSPCS)*. Cairns: IEEE, 2018, pp. 1-5. DOI 10.1109/ICSPCS.2018.8631767.
- [8] PIYARATNA, S., N. DUONG, J. CARR, D. BIRD, S. KENNEDY and A. UDINA. Digital RF Processing System for Hardware-in-the-Loop Simulation. In: *2013 International Conference on Radar*. Adelaide: IEEE, 2013, pp. 554-559. DOI 10.1109/RADAR.2013.6652048.
- [9] MOUDGALYA, A., P.J. MORRIS and C.V. GIRIRAJA. Motion Compensation on Range Doppler Algorithm for Airborne SAR. In: *2018 International Conference on Advances in Computing, Communications and Informatics (ICACCI)*. Bangalore: IEEE, 2018, pp. 1303-1306. DOI 10.1109/ICACCI.2018.8554378.
- [10] JIAGUO, L. *Design Technology of Synthetic Aperture Radar*. Wiley-IEEE Press, 2019. ISBN 978-1-119-56467-0.
- [11] CUMMING, I.G. and F.H. WONG. *Digital Processing of Synthetic Aperture Radar Data*. Norwood: Artech House, 2005. ISBN 978-1-58053-058-3.
- [12] LONG, S., Z. HONG-RONG, T. YUE-SHENG and Z. CHANG-YAO. Research on Deceptive Jamming Technologies against SAR. In: *2009 2nd Asian-Pacific Conference on Synthetic Aperture Radar*. Xi'an: IEEE, 2009, pp. 521-525. DOI 10.1109/APSAR.2009.5374233.
- [13] LIN, X., P. LIU and G. XUE. Fast Generation of SAR Deceptive Jamming Signal Based on Inverse Range Doppler Algorithm. In: *IET International Radar Conference 2013*. Xi'an: IET, 2013, pp. 1-4. DOI 10.1049/cp.2013.0465.
- [14] KESHAVAMURTHY, B., A. NARASIMHA, A.S. ASIF AHMAD, N. MAHESH, and M.N. SUMA. Hardware-in-Loop Simulation of a White-Fi System Utilizing the TV White Spaces in India Enabling Cost-Effective Rural Broadband to Ensure Total Internet Adoption. In: *2016 5th International Conference on Wireless Networks and Embedded Systems (WECON)*. Rajpura: IEEE, 2016, pp. 1-7. DOI 10.1109/WECON.2016.7993468.

-
- [15] BARLINDHAUG, S., I. HOLM-OLSEN and H. TØMMERVIK. Monitoring Archaeological Sites in a Changing Landscape - Using Multitemporal Satellite Remote Sensing as an 'Early Warning' Method for Detecting Regrowth Processes. *Archaeological Prospection*, 2007, **14**(4), pp. 231-244. DOI 10.1002/arp.307.
- [16] XIONG, Z., R. RADHAKRISHNAN, A. DIVAKARAN, Y. RUI and T. HUANG. *A Unified Framework for Video Indexing, Summarization, Browsing, and Retrieval, with Applications to Consumer and Surveillance Video*. Boston: Academic Press, 2005. ISBN 0-12-369387-X.
- [17] SMITH, M.A. and T. CHEN. Image and Video Indexing and Retrieval. In: A.L. BOVIK, ed. *Handbook of Image and Video Processing*. 2nd ed. Burlington: Academic Press, 2005, pp. 993-1012. ISBN 978-0-12-119792-1.